Predicting Orbital Resonance of 2867 Šteins Using the Yarkovsky Effect[1]

Will Rosenberg

Esteban Herrera-Vendrell*[2]

Raymond Nucuta*

Karsen Wahal*

Sarthak Bhardwaj

William Bryce Gallie

Advisor: Paul McClernon

BASIS Scottsdale, Scottsdale, Arizona

[1] All code for this paper can be found here: https://github.com/rnucuta/orbitalResonanceResearch.

[2] Students with an asterisk have the same contribution.

Summary

While gravitational forces have the largest impact on asteroid orbit determination, thermal forces such as the Yarkovsky and YORP effects also perturb orbits. Creating the question: will the Yarkovsky Effect push Šteins into a Kirkwood Gap within 50,000 years? We hypothesize that the Yarkovsky effect will push 2867 Šteins into a Kirkwood gap within 50,000 years because Šteins falls into the range of asteroid sizes that the Yarkovsky Effect significantly affects (15). We computationally generate a thermal map of the asteroid 2867 Šteins to approximate the Yarkovsky force and YORP torque on Šteins. Then, the orbit of Šteins is modeled to determine whether thermal effects push Šteins into a Kirkwood gap. The thermal map is based on the Simple Thermal Model outlined by Rozitis and Green (1), assuming thermal properties from the Rosetta flyby mission. Analysis of the thermal map yields an average Yarkovsky force parallel to velocity of -0.714 N, and an acceleration of $-5.22 \cdot 10^{-15}$ m/s^2. The torque parallel to the angular velocity due to the YORP effect is 4.680 N·m, with an angular acceleration of $1.217 \cdot 10^{-20}$ rad/s^2. The Yarkovsky force is inputted into NASA's GMAT to measure the change to Šteins' orbit due to the Yarkovsky effect. The force is found to alter Šteins's orbit, but does not yield a significant probability of transferring Šteins to a Kirkwood gap. We find that the Yarkovsky force decays the semi-major axis of Šteins by 16.4 km in 242.2 years, and up to 5,365 km in 50,000 years within 95% confidence.

Introduction

In recent decades, scientists have placed an increased focus on the motion of asteroids within the asteroid belt. While it was originally believed that asteroids were primarily affected by gravitational forces, recent research reveals that other forces due to the Yarkovsky effect play a role in an asteroid's trajectory. Discovered by Polish engineer Ivan Yarkovsky, the Yarkovsky effect is a force caused by the asymmetrical emission of electromagnetic radiation due to thermal radiation from rotating bodies in space (3). As the asteroid rotates, the sun heats it, and the radiation absorbed by the asteroid is re-emitted in a different direction because of the delay between absorption and re-emission (3). This re-emission generates a recoil force in the opposite direction of emission of electromagnetic radiation (3). Although the Yarkovsky effect exists in all astronomical bodies, it is typically observed most prominently in asteroids because asteroids have the highest surface area to mass ratios in regard to natural astronomical bodies (15).

Existing literature indicates that over long periods of time, the Yarkovsky effect can perturb the orbit of an asteroid. However, research on the Yarkovsky effect remains small-scale; this paper applies this effect to 2867 Šteins. We hope to answer the question: will the Yarkovsky Effect push 2867 Šteins into a Kirkwood Gap within 50,000 years? Through the use of computer modeling, we investigate whether the Yarkovsky effect will push 2867 Šteins into a Kirkwood Gap within a 50,000-year timespan. We hypothesize that the Yarkovsky effect will push 2867 Šteins into a Kirkwood gap because Šteins falls into the range of asteroid sizes that are significantly affected by the Yarkovsky Effect. 2867 Šteins is an E type, non-family, inner belt asteroid that orbits the sun with a semi-major axis of 2.3633 AU and an orbital period of 1327 days (4). Šteins is close to a Kirkwood Gap, which is a region of the asteroid belt largely devoid of asteroids. These gaps exist at 2.06 AU, 2.5 AU, 2.82 AU, 2.95 AU and 3.27 AU from the sun; bodies with semi-major axes that reside within these gaps are in orbital resonance with Jupiter, resulting in a gravity assist from Jupiter that eventually propels the body out of the asteroid belt and potentially into the inner solar system (5). 2867 Šteins' distance to a Kirkwood gap of 0.30 AU makes it possible that Šteins might slip into one. In this paper, we determine what effect, if any, the Yarkovsky effect has on pushing Šteins into a Kirkwood gap by simulating the asteroid's orbit.

Solar radiation pressure is ignored because previous research reveals that it does not significantly alter the semi-major axis of an asteroid's orbit when considered with the Yarkovsky effect (2). *Eqn. 1* represents the Yarkovsky force over the surface of the asteroid (13):

$$\vec{f} = -\frac{2\sigma}{3c}\int_{\sum} \varepsilon T^4 \, \vec{n} \, ds \qquad \text{(Eqn. 1)}$$

where *c* is the speed of light, σ is the Stefan-Boltzmann constant, ε is the emissivity of the surface, *T* is the temperature of the surface, n is the normal vector to the surface, and *ds* is the differential area element.

YORP, or the Yarkovsky–O'Keefe–Radzievskii–Paddack effect, is the torque that the Yarkovsky effect creates (3). When the Yarkovsky effect acts on asymmetrical bodies, it creates a net torque, causing the body to accelerate about an axis (3). This spin continuously changes the Yarkovsky force, as the rotation state (axis of rotation, period of rotation, etc.) largely determines the direction and magnitude of the Yarkovsky force (3). *Eqn. 2* represents the YORP torque generated over the surface of the asteroid (13):

$$\vec{T} = -\frac{2\sigma}{3c}\int_{\sum} T^4\,\vec{x} \times \vec{n}\,ds \qquad \text{(Eqn. 2)}$$

where *x* is the vector from the center of mass of the body to the surface. Over time, this torque can significantly change the spin state of an asteroid, which impacts the Yarkovsky force. However, the magnitude of the angular acceleration due to the Yarkovsky effect on 2867 Šteins is sufficiently small that the change in spin state is insignificant.

The surface temperature of 2867 Šteins is required to quantify the Yarkovsky effect. As a result, the first step is to create a thermal map of the asteroid. Rozitis and Green (1) is used as a template. A stereolithography (STL) file of Šteins is divided into 1500 triangular facets, where each facet represents a portion of Šteins' surface. The thermal map is partitioned into 50 depth-steps per facet and 400 time-steps per rotation.

Figure 1. 3D model of 2867 Šteins

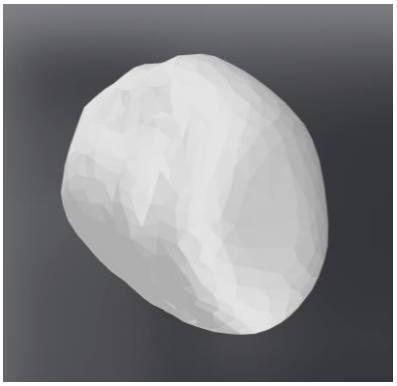

The goal is to determine the temperature of each facet at any given point in the rotation. For simplicity, only 1-D heat conduction is considered, similar to Rozitis and Green (1). The thermal map is created based upon the surface boundary condition imposed by conservation of energy,

$$\left(1-A_B\right)\left(\left[S(\tau)\right]\psi(\tau)\,F_{SUN}\right)+\frac{\Gamma}{\sqrt{4\pi P_{ROT}}}\left(\frac{\partial T}{\partial z}\right)_{z=0}-\varepsilon\sigma T^4_{z=0}=0 \qquad \text{(Eqn. 3)}$$

where A_B is the Bond albedo, ε is the emissivity, σ is the Stefan–Boltzmann constant, $S(\tau)$ indicates whether the facet is shadowed with a 0 or a 1, Γ represents the thermal inertia, ψ(τ) returns the cosine of the sun illumination angle, and F_{SUN} is the integrated solar flux at the distance of the object, which is given by $(1367/r^2)W/m^2$ where r is the heliocentric distance of the planetary body in AU. Unlike Rozitis and Green (1), F_{SCAT} and F_{RAD} are ignored because Šteins is primarily convex, so the intensity of the light reflected and reabsorbed by the asteroid is significantly smaller than the light from the sun. z is the normalized depth variable given by

$$z = \frac{x}{\iota_{2\pi}} \qquad \textit{(Eqn. 4)}$$

and τ is the normalized time variable, given by

$$\tau = \frac{t}{P_{ROT}} \qquad \textit{(Eqn. 5)}$$

Based on these relationships, the initial mean surface temperature of each facet is found using *Eqn. 6*.

$$\left\langle T_{z=0} \right\rangle_1 = \left(\frac{\left(1 - A_B\right)}{\varepsilon\sigma} \right)^{1/4} \frac{\int_{\tau=0}^{1} \left(\left[1 - S(\tau)\right] \psi(\tau) F_{SUN} \right)^{1/4} \mathrm{d}\tau}{\int_{\tau=0}^{1} \mathrm{d}\tau} \qquad \textit{(Eqn. 6)}$$

S(τ) determines which facets receive light by determining whether any other facets block light from reaching it. To calculate $\psi(\tau)$, the scalar product of the vector normal to each facet and the vector representing the sun's ray is used to find $\cos(\theta)$. The results for $T_{z=0}$ give the mean surface temperature of each facet over one period, which is equated to the temperatures of each respective facet and its depth steps at τ = 0. Using *Eqn. 3*, the temperature after one time-step is determined. The solution for $T_{z=0}$ represents the surface temperature of each facet at τ = 1, respectively. Given the surface temperature at τ = 1, the temperature at τ = 1 is calculated at varying depth steps. The equation

$$T_{i,\,j+1} = T_{i,\,j} + \frac{1}{4\pi} \frac{\delta\tau}{(\delta z)^2} \left[T_{i+1,\,j} - 2T_{i,j} + T_{i-1,j} \right] \qquad \textit{(Eqn. 7)}$$

is used where i = 1 to n depth-steps and j = 1 to m time-steps. *Eqn. 7* is a difference equation developed to locally approximate the differential equation for 1-D heat conduction, given by:

$$\frac{\partial T}{\partial \tau} = \frac{1}{4\pi} \frac{\partial^2 T}{\partial z^2} \qquad \textit{(Eqn. 8)}$$

The last depth step is set equal to the second-to-last depth step in order to satisfy the internal boundary condition

$$\left(\frac{\partial T}{\partial z}\right)_{z\to\infty} \to 0 \qquad \textit{(Eqn. 9)}$$

This process is repeated for at least ten full rotations, ultimately giving the temperature of each facet at any given time-step.

The thermal map is used to calculate the Yarkovsky effect. This force is simulated within NASA's GMAT Orbital Determination software to determine the resulting change in the orbit of Šteins.

Results

The model is implemented at six different positions along the orbit, returning a force vector and torque vector at each. The torque parallel to the angular velocity is represented by τ_P. Each force vector is broken into three directions: tangent to the velocity (F_T), perpendicular to the orbital plane (F_P), and perpendicular to the velocity and in the orbital plane (F_O). These three directions create a new coordinate axis that the force is defined on. The new coordinate axis accounts for the changing position in the orbit by defining the force vector relative to the velocity vector. Using this coordinate axis, each force is simulated for one-sixth of 2867 Šteins' orbit for 242.2 years. The Yarkovsky force and torque results for each respective date are documented in *Table 2*:

Table 2. Yarkovsky Force and Torque vectors.

Date	**Position Relative to the Sun (*AU*)**	**Force (*N*)**	**τ_P ($N \cdot m$)**	**F_T (*N*)**	**F_P (*N*)**	**F_O (*N*)**
March 30, 2014	x = -0.530 y = 2.593 z = 0.334	x = 0.306 y = 1.236 z = 1.086	-0.056	-0.344	0.992	1.304
November 6, 2014	x = -2.226 y = 1.412 z = 0.461	x = -0.643 y = 1.060 z = 1.221	-15.027	-0.636	1.008	1.269
June 15, 2015	x = -2.290 y = -0.758 z = 0.255	x = -1.670 y = 0.200 z = 1.025	12.153	-1.050	0.753	1.487
January 22, 2016	x =-0.2421 y = -2.069 z = -0.171	x = -1.199 z = -2.217 y = -0.641	4.637	-1.063	-0.584	2.301
August 30, 2016	x = 1.959 y = -0.580 z = -0.340	x = 1.987 y = -1.583 z = -1.592	3.227	-0.812	-1.131	2.656
April 8, 2017	x = 1.520 y = 1.855 z = -0.034	x = 1.515 y = 0.797 z = 0.237	23.145	-0.377	0.371	1.646

The resulting thermal map for 2867 Šteins on June 15, 2015, is shown in *Figure 2*.

Figure 2. Thermal Map of 2867 Šteins

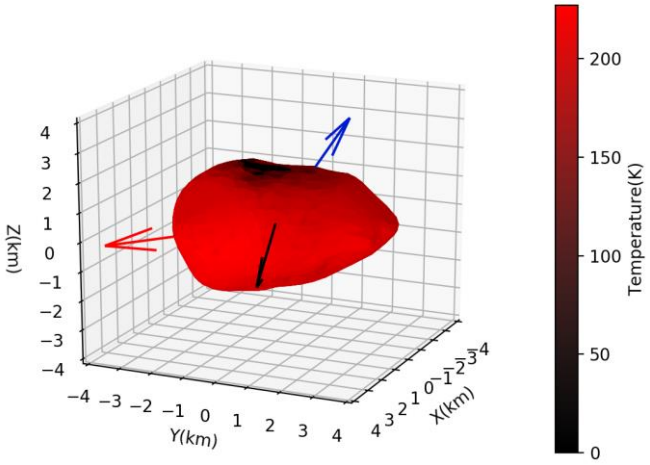

In *Fig. 2*, the temperature of each facet is represented through a linear color gradient. The black vector points towards the sun, the red vector represents the direction of the velocity of the asteroid, and the blue vector displays the direction of the final Yarkovsky force vector. The off-center locations of the hottest facets shift the Yarkovsky force vector off-center against the asteroid's direction of motion.

The average tangential Yarkovsky force is -0.714 N, and the average tangential acceleration is $-5.22 \cdot 10^{-15}$ m/s^2. The average torque in the direction of angular momentum is 4.680 N·m, and the average angular acceleration is $1.217 \cdot 10^{-20}$ rad/s^2.

The results from GMAT reveal that 2867 Šteins' semi-major axis decays 16.4 km in 242.2 years. The magnitude and direction of the Yarkovsky force at different points in Šteins' orbit are illustrated in *Fig. 3*.

Figure 3. 2867 Šteins' Orbit Diagram

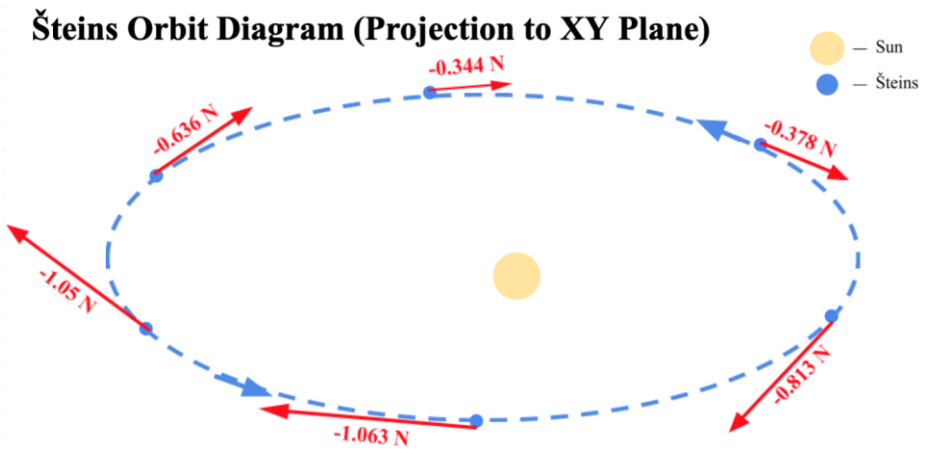

The changes in Šteins' semi-major axis, inclination, and eccentricity over the documented time period of 242.2 years are shown in *Figure 4.*

Figure 4. Orbital Elements Versus Time Graphs

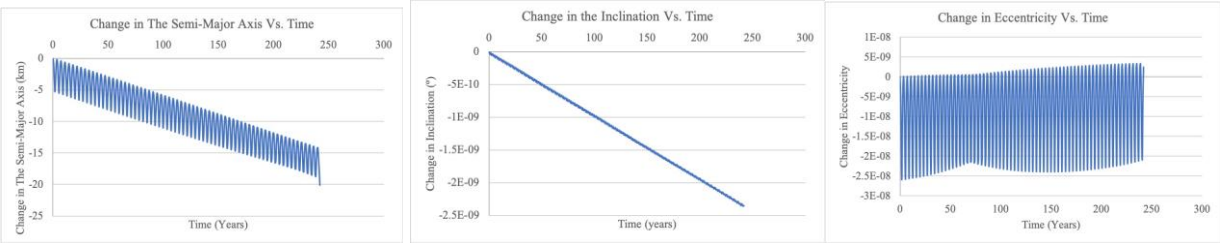

Using a forecast function and exponential smoothing, the changes in the semi-major axis, inclination, and eccentricity are predicted over longer time spans with a 95% confidence interval documented in *Table 3*.

Table 3. Orbital results of The Yarkovsky Effect.

Time (years)	Change in the semi-major axis (km)	95% Confidence Radius	Change in Inclination (°)	95% Confidence Radius	Change in Eccentricity	95% Confidence Radius
250	-17.01	0.31	-2.4E-09	3.1E-12	3.3E-09	7.1E-10
500	-34.8	2.1	-4.8E-09	2.2E-11	4.6E-09	4.9E-09
1000	-59.9	6.3	-9.7E-09	6.3E-11	-7.5E-09	1.5E-08
10000	-595	214	-9.7E-08	2.0E-09	1.5E-07	5.0E-07
50000	-2950	2415	-4.8E-07	2.2E-08	7.4E-07	5.6E-06

Discussion

The resulting direction of the tangential force at each position matches the hypothesized direction, against the motion of the asteroid. However, the magnitude of the tangential force varies between positions, with a range of 0.719 N. We hypothesize that this variation is due to variation in the asteroid's position in the z-direction, distance from the sun, and shape. However, more investigation is necessary to analyze the precise causes of this variation.

The results also indicate with 95% confidence that within 50,000 years, 2867 Šteins does not enter a Kirkwood Gap. After 50,000 years, Šteins is predicted to move 0.0065% of the 0.3033 AU necessary to enter a Kirkwood Gap. If Šteins follows the lower bound of the confidence interval, Šteins will move 0.012% of the 0.3033 AU necessary to enter a Kirkwood Gap. Thus, the minimal change in Šteins' semi-major axis provides evidence that asteroids with sizes comparable to Šteins are not heavily influenced by

the Yarkovsky effect. However, the Yarkovsky force does have a significant effect on the orbit of Šteins, decaying its semi-major axis by 16.4 km after 242.2 years and by up to 5,365 km in 50,000 years. This reinforces the notion that the Yarkovsky effect needs to be considered for asteroids in the sub ~20 km mean diameter range (15). Although the Yarkovsky effect affects the orbit of 2867 Šteins, it is not a significant force on the orbit of Šteins unless considered in the scale of orbital maneuvers. Therefore, we reject our hypothesis that the Yarkovsky effect will push 2867 Šteins into a Kirkwood within 50,000-years. Future studies can analyze the seasonal effect and include more specific factors that affect the Yarkovsky force, such as the scattering and reabsorption of light.

Methods

All code is written in Python using a class-based subsumption architecture structure. The basic structure of the code is as follows: using physical properties of 2867 Šteins, the code outputs a thermal map that generates a Yarkovsky vector that is inputted into NASA's GMAT orbital simulation software.

The asteroid radius, Bond albedo, density, mass, thermal conductivity, thermal inertia, position, rotation period, and spin are major factors in determining the Yarkovsky effect on 2867 Šteins. The physical parameters of Šteins are well-known and documented in *Table 1*. However, some values, such as mass and thermal conductivity, are not explicitly documented. The thermal conductivity is found because Šteins is known to have a similar surface composition as enstatite (7). Given that enstatite has a thermal conductivity of approximately 4.5 W·m/K (10), the thermal conductivity of Šteins is approximated as 4.5 W·m/K. The mass is found by multiplying the recorded density and volume of Šteins.

Table 1. Physical Properties of the Asteroid 2867 Šteins

Property	**Value**
Mean Radius (9)	2.7 km
Bond albedo (10)	0.24
Density (9)	1800 kg/m^3
Mass (9)	$1.368 \cdot 10^{14}$ kg
Thermal Conductivity (11)	4.5 W·m/K
Thermal Inertia (12)	110 $J/m^2 \cdot K \cdot s^{1/2}$
Emissivity (12)	0.73
Position (13)	N/A
Rotation Period (12)	6.0468 hours
Spin (7)	(250.0°, −89.0°) in ecliptic coordinates

A *Rays* class representing vectors of sunlight hitting the asteroid is created first. In order to determine which facets are shadowed, the class *Shadowing* is created with two conditions. First, all facets that face directly away from the sun are shadowed. This is found by comparing the normal vector of each

facet to the vectors of sunlight. Second, shadowing is detected in the remaining facets by determining which facets the rays intersect. This is found by calculating the signed volume of various tetrahedrons. These tetrahedrons have 5 points, including the 3 vertices of the facet and 2 random points on the ray. Once it is determined which rays intersect which facets, the code then determines which facet is intersected first using the parametric equation for the ray. If a ray of light intersects one facet before another, then the other facet that would have been hit by that ray of light is "shadowed."

One addition to the shadowing class is the angle functions *phi()* and *orient()*. *orient()* orients the asteroid's north and south poles in the STL file in the direction that they are oriented in 3-D space, taking the XY-axis as the ecliptic plane. *phi()* returns the cosine of the angles between the normal vectors of each facet and the rays from the sun by dividing the dot product of the normal vectors and the sun rays by the product of the lengths of both vectors. These methods are implemented in the shadowing, angle, and thermal map code.

The thermal map code imports the *Rays* and *Shadowing* classes. The methods described in the **Introduction** are used to determine the temperature of each facet at different times. The resulting thermal map is shown in *Figure 2*.

Each point in an asteroid's orbit has a unique Yarkovsky and YORP vector assigned to it, based on its distance from and orientation to the sun. In order to determine the Yarkovsky force vector, the thermal map of Šteins is imported, and the force due to thermal emission on the asteroid is evaluated at each time step using the approach outlined in *Eqn. 1*. The surface integral represents the net force on the asteroid at a single time step. Iterating over the entire rotation and averaging these values yields the representative Yarkovsky force vector for that position in space. A similar approach is taken for the YORP vector, using *Eqn. 2*. The torques for all facets are taken with respect to the center of mass of the asteroid, which is given in the mass properties of the STL file. These processes are repeated for six locations to simulate the variation in the force throughout the orbit, resulting in six different vectors.

To determine the change to 2867 Šteins' orbit, NASA's GMAT software is used. The asteroid is simulated as a spacecraft with the Yarkovsky vector as the thrust vector. Each of the six different vectors is inputted at their respective locations. The simulation is run for 242.2 years, using the integrator RungeKutta89 and an initial step size of 10. These results reveal the change in the orbit of Šteins due to the Yarkovsky effect after 242.2 years. A forecast function is used on the resulting data to extrapolate the results to longer periods of time. All astronomical measurements are taken and determined in heliocentric ecliptic cartesian coordinates.

Acknowledgements

The theory behind the Yarkovsky effect in this paper was aided by the guidance of Dr. Simon Green of the Open University. We deeply appreciate the guidance of Dr. Green and the JEI editorial staff.

References

1. Rozitis, B., and S. F. Green. “Directional Characteristics of Thermal-Infrared Beaming from Atmosphereless Planetary Surfaces - a New Thermophysical Model.” *Monthly Notices of the Royal Astronomical Society*, vol. 415, no. 3, June 2011, pp. 2042–2062., doi:10.1111/j.1365-2966.2011.18718.x.
2. Deo, S.n., and B.s. Kushvah. “Yarkovsky Effect and Solar Radiation Pressure on the Orbital Dynamics of the Asteroid (101955) Bennu.” *Astronomy and Computing*, vol. 20, 2017, pp. 97–104., doi:10.1016/j.ascom.2017.07.002.
3. Vokrouhlicky, David, and William F. Bottke. “Yarkovsky and YORP Effects.” Scholarpedia, Scholarpedia, 2012, www.scholarpedia.org/article/Yarkovsky_and_YORP_effects.
4. “ASTEROID (2867) Šteins.” *ESA Science & Technology - Asteroid (2867) Šteins*, European Space Agency, 1 Sept. 2019, sci.esa.int/web/rosetta/-/43356-2867-Šteins.
5. “Kirkwood Gap: Facts, Information, History & Definition.” *The Nine Planets*, The Nine Planets, 5 Mar. 2020, nineplanets.org/kirkwood-gap/.
6. Lamy, P L, et al. “Asteroid 2867 Šteins - II. Multi-Telescope Visible Observations, Shape Reconstruction, and Rotational State.” *Astronomy & Astrophysics*, vol. 487, no. 3, Sept. 2008, pp. 1179–1185., doi:https://doi.org/10.1051/0004-6361:20078995.
7. Barucci, M. A., et al. “Asteroids 2867 Šteins and 21 Lutetia: Surface Composition from Far Infrared Observations with the Spitzer Space Telescope.” *Astronomy & Astrophysics*, vol. 477, no. 2, Dec. 2007, pp. 665–670., doi:10.1051/0004-6361:20078085.
8. Farnham, T.L., “PLATE SHAPE MODEL OF ASTEROID Šteins V1.0.” *RO-A-OSINAC/OSIWAC-5-Šteins-SHAPE-V1.0*, NASA Planetary Data System, 2013.
9. Spjuth, S., et al. “Disk-Resolved Photometry of Asteroid (2867) Šteins.” *Icarus*, vol. 221, no. 2, Nov. 2012, pp. 1101–1118., doi:10.1016/j.icarus.2012.06.021.
10. Sj, C. P. Opeil, et al. “Stony Meteorite Thermal Properties and Their Relationship with Meteorite Chemical and Physical States.” *Meteoritics & Planetary Science*, vol. 47, no. 3, 2012, pp. 319–329., doi:10.1111/j.1945-5100.2012.01331.x.

11. Leyrat, C., et al. “Thermal Properties of the Asteroid (2867) Šteins as Observed by VIRTIS/Rosetta.” *Astronomy & Astrophysics*, vol. 531, 1 May 2011, doi:10.1051/0004-6361/201116529.
12. Park, Ryan, and Alan Chamberlin., “HORIZONS Web-Interface.” *JPL’s Horizon system*. 3 May 2020.
13. Pelaez, Jesus, et al. “A New Approach on the Long Term Dynamics of NEO's Under Yarkovsky Effect.” *Advances in the Astronautical Sciences* , vol. 140, no. 11-440, Dec. 2011, doi: 2011AdAnS.140..440P .
14. Bottke, William F., et al. “The Effect of Yarkovsky Thermal Forces on the Dynamical Evolution of Asteroids and Meteoroids.” *Asteroids III*, Mar. 2002, pp. 395–408., doi:2002aste.book..395B.
15. Bottke, William F., et al. “THE YARKOVSKY AND YORP EFFECTS: Implications for Asteroid Dynamics.” *Annual Review of Earth and Planetary Sciences*, vol. 34, no. 1, 16 Jan. 2006, pp. 157–191., doi:10.1146/annurev.earth.34.031405.125154.